Hyperbranched Polyester Based on the Core + AB_2 Approach: Synthesis and Structural Investigation

Kishore K. Jena, Ramanuj Narayan, K. V. S. N. Raju

Organic Coatings and Polymers Division, Indian Institute of Chemical Technology, Hyderabad 500 607, India

Received 13 August 2009; accepted 18 February 2010
DOI 10.1002/app.32297
Published online 19 May 2010 in Wiley InterScience (www.interscience.wiley.com).

ABSTRACT: In this study, structural buildup studies during the synthesis of fifth-generation hyperbranched polyesters (HBPs) from 2-bis(hydroxymethyl) propionic acid (AB_2) and glycerol (core) by a one-pot process were undertaken. The variations in the degree of polymerization, hydrogen bonding, rheology, and role of cyclization were studied by NMR, Fourier transform infrared spectroscopy, rheometry, and matrix-assisted laser desorption/ionization time of flight. The degree of branching was calculated at different time intervals from the integral peak areas of the terminal, linear, and dendritic repeating units of ^{1}H-NMR and ^{13}C-NMR. The rheology study performed on the HBPs revealed that hydrogen bonds played an important role in the determination of the melt viscosity. © 2010 Wiley Periodicals, Inc. J Appl Polym Sci 118: 280–290, 2010

Key words: hyperbranched; FT-IR; MALDI; NMR

INTRODUCTION

In recent years, widespread research efforts have been made in the development of the dendritic (D) class of macromolecules for various applications because of their unique chemical and physical properties. Their properties are, to a large extent, dependent on the number and nature of their end groups.[1–6] Dendrons, dendrimers, and hyperbranched (HB) polymers consisting of successive branching units belong to this class of macromolecules. The dendrons and dendrimers exhibit a well-controlled size, shape, and molecular weight, whereas the hyperbranched polymers exhibits a random branched structure. Among them, HB polymers have drawn considerable interest recently because of their low-cost, simple, one-pot synthetic procedure with almost similar or comparable properties compared to dendrimers.[7–12]

HB polymers are in general based on AB_x monomers ($x \geq 2$), and each repeat unit constitutes a branching point, such as linear (L), terminal (T), or D, and has many end groups in comparison with L polymers.[13,14] These polymers exhibit properties such as increased solubility, lower viscosity in solution and the molten state, chain-end effects, and a lack of entanglements; thereby, these significantly differ from L polymers because of their molecular architecture and the nature of their end groups.[15–19]

Generally, HB polymers with Hydroxyl Terminal groups have been synthesized by the polycondensation of activated derivatives of 2,2-bis(hydroxymethyl) propionic acid (bis-MPA) with trimethylol propane or ethoxylated pentaerythritol with the core + AB_2 approach.[20–23] Recently, fourth- and fifth-generation HB polyesters have been prepared with pentaerythritol and bis-MPA by one-step and step by step and have been characterized by various techniques.[24] A glycerol (GLY) core has been used to synthesize hyperbranched polyesters (HBPs) with dimethyl-5-(2-hydroxyethoxy) isophthalic acid[25] (AB_2) and adipic acid,[17,26] with the AB_2 + B_3 strategy. Earlier, for the first time, we reported third-generation HBPs with GLY as a core through the core + AB_2 approach and compared it with HBPs synthesized with other cores, such as trimethylol propane and pentaerythritol; we also used molecular simulations for this purpose.[27] However, until now, no work has been published dealing with structural investigation of fifth-generation HBPs prepared with GLY as a core. The conditions, including molar ratio, reaction time, and temperature, and the reactivity of the end groups and so on affect the formation of HBPs. There are some products based on bis-MPA with different cores are available commercially, but their structural data during synthesis has not been reported anywhere. The aim of this study was to investigate the structural buildup in the formation of HBPs with GLY and bis-MPA at different reaction times. Their properties, including the degree of branching (DB), hydrogen bonding, role of cyclization, degree of polymerization (DP), and rheology, were studied with different instrumental techniques.

Correspondence to: K. V. S. N. Raju (kvsnraju@iict.res.in or drkvsnraju@gmail.com).

Contract grant sponsors: Council of Scientific and Industrial Research (New Delhi, India; a research fellowship.

EXPERIMENTAL

Materials

2-Bismethylol propionic acid (bis-MPA) and titanium tetraisopropoxide were purchased from Aldrich (Milwaukee, WI). GLY and dimethylformamide were procured from Qualigens (Mumbai, India). Tetrahydrofuran (THF) and sulfur-free toluenes were purchased from S. D. Fine Chemicals (Mumbai, India). All of these reagents were used without any further purification.

Synthesis of the HBPs

The HBPs were prepared with the divergent approach in a single-step melt condensation reaction with bis-MPA and a GLY core with a molar ratio of 1 : 93. The GLY was charged to bis-MPA kept in a four-necked, round-bottom flask placed over an isomantle bath and equipped with a thermometer, mechanical stirrer, nitrogen inlet, and Dean–Stark apparatus. The reaction mixture was slowly heated to 190°C. After the reactants were completely melted, the temperature was maintained between 190 and 200°C with a continuous nitrogen flow for about 72 h. Titanium tetraisopropoxide (0.05 wt % on the basis of the weight of bis-MPA) was used as the catalyst for the esterification. We monitored the reaction periodically by determining the acid value titrimetically. The HBPs samples were collected at different intervals, 3, 5, 15, 30, 48, and 72 h, to investigate the structural buildup of HBPs with different techniques. Usually, gelation is encountered during the synthesis of these polyesters, but with proper control of the temperature and catalyst concentration, we prepared these polyesters without gelation.

Characterization and measurements

The molecular weights of the HBPs were determined with gel permeation chromatography (GPC; Shimadzu LC 10ATVP series, Japan) with a refractive index detector. Samples were prepared in THF solvent at a 5 mg/mL concentration. The flow rate of the mobile phase was kept at 1.0 mL/min. The instrument was calibrated with polystyrene standards.[7] The ^{1}H-NMR and ^{13}C-NMR spectra were recorded on a Varian VXR Unity 200-MHz spectrometer and a Bruker UXNMR 300-MHz spectrometer in hexadeuterated dimethyl sulfoxide (DMSO-d_6) with trimethylsilane as an internal standard. The matrix-assisted laser desorption/ionization (MALDI) time-of-flight (TOF) mass spectra were recorded with a Kompact MALDI SEQ laser desorption TOF mass spectrometer (Kratos Analytical, Manchester, England) equipped with a pulsed nitrogen laser (λ_{max} = 337 nm, pulse width = 3 ns). Ions were accelerated into the analyzer at a voltage of 20 kV. The sample spots were irradiated just above the threshold with L mode with pulsed extraction (delayed extraction). Thus, the laser power (irradiance) used to produce a good mass spectrum was analyte-dependent. The L mode was chosen over the reflector mode to maximize the signal intensity because resolving power was sufficient to differentiate the observed oligomers. All of the mass spectra shown here were accumulated over 50 laser shots across the sample spot. The matrix used was 2-(4-hydroxyphenylazo) benzoic acid (Sigma, St. Louis, MO) at a 10 mg/mL concentration in THF solvent. The samples were prepared in THF solvent at a 1 mg/mL concentration. To make an analyte/matrix deposit, typically, 0.3 μL of the analyte solution was placed on a stainless steel sample slide (part no. D 3665 TA, Kratos Instruments), and the solvent was removed by forced-air evaporation at room temperature. Subsequently, 0.3 μL of the matrix solution was placed above the sample spot covering the analyte film, and again, the solvent was removed by forced-air evaporation at room temperature. THF diluted drops of HBPs samples were spread on dry KBr discs and were vacuum-dried at 80°C for a long period of time to reduce the levels of solvent and adsorbed water in the samples before Fourier transform infrared (FTIR) spectra were recorded

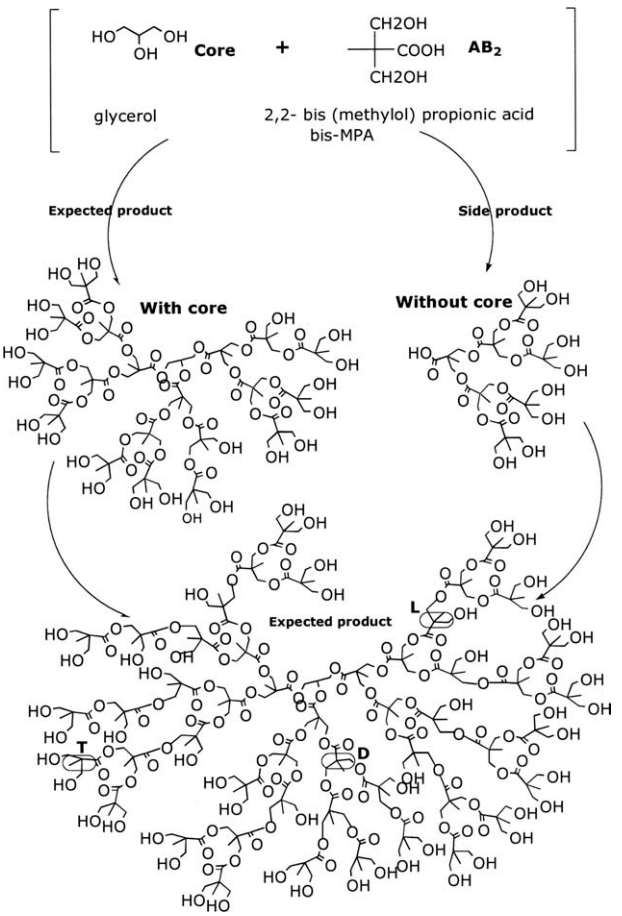

Scheme 1 Idealized structure of the HBPs prepared from GLY and bis-MPA (expected product and side product).

TABLE I
GPC Data of Different HBPs

Sample	M_w (g/mol)[a]	M_n (g/mol)[a]	PDI[a]
5 h	1914	1182	1.61
15 h	2080	1378	1.50
30 h	2744	1842	1.48

M_w = weight-average molecular weight.
[a] M_w and M_n were calculated from GPC.

under ambient conditions on a Thermo Nicolet Nexus 670 spectrometer. IR data was obtained with the Thermo Nicolet Nexus 670 spectrophotometer between 4000 and 400 cm^{-1} at a resolution of 4 cm^{-1}. The analysis and peak deconvolution of N—H and C=O bands were performed on Origin 6.0 software with the peaks considered as Gaussian with a number of iteration to get the best-fit Gaussian peaks. The maximum error associated with the fit was estimated to be less than 4%. The melt viscosity of the HBPs samples was determined with an Anton Paar Physica MCR 51 rheometer (Graz, Austria) in cup and bop geometry at 30, 40, 50, and 60°C and from 10° to a 10^2 s^{-1} shear rate.

RESULTS AND DISCUSSION

An idealized structure of fifth-generation HBPs is shown in Scheme 1. A series of HBPs synthesized at different time intervals with bis-MPA and a GLY core were characterized with different techniques for the structural buildup investigation. The molecular weight of the synthesized HBPs was measured with GPC, whereas the composition and structure were analyzed with ^{1}H-NMR and ^{13}C-NMR spectroscopy. MALDI-TOF mass spectrometry was used to calculate and analyze the extent of cyclization and DP, and hydrogen-bonding information was obtained from FTIR spectroscopy.

GPC analysis

GPC was used to determine the molar masses and molar mass distributions of the HBPs, and the results are shown in Table I. The obtained molar masses were generally lower than the corresponding theoretical molar masses. This was probably because all of the investigated samples had a highly branched molecular architecture. The heterogeneous nature of the HBPs could be observed from the polydispersity index (PDI) data.

TABLE II
^{1}H-NMR and ^{13}C-NMR Analysis of the HBPs

	DB_{Frey} (%)		$DB_{Frechet}$ (%)	
Sample	^{13}C-NMR (C=O)	^{1}H-NMR (—CH_3)	^{13}C-NMR (C=O)	^{1}H-NMR (—CH_3)
3 h	20.5	30.3	55.8	55.0
5 h	22.9	35.4	57.5	59.5
15 h	25.7	40.0	62.6	61.7
30 h	37.5	43.0	69.5	63.7
48 h	46.5	50.0	71.8	67.9
72 h	57.3	53.7	74.8	71.5

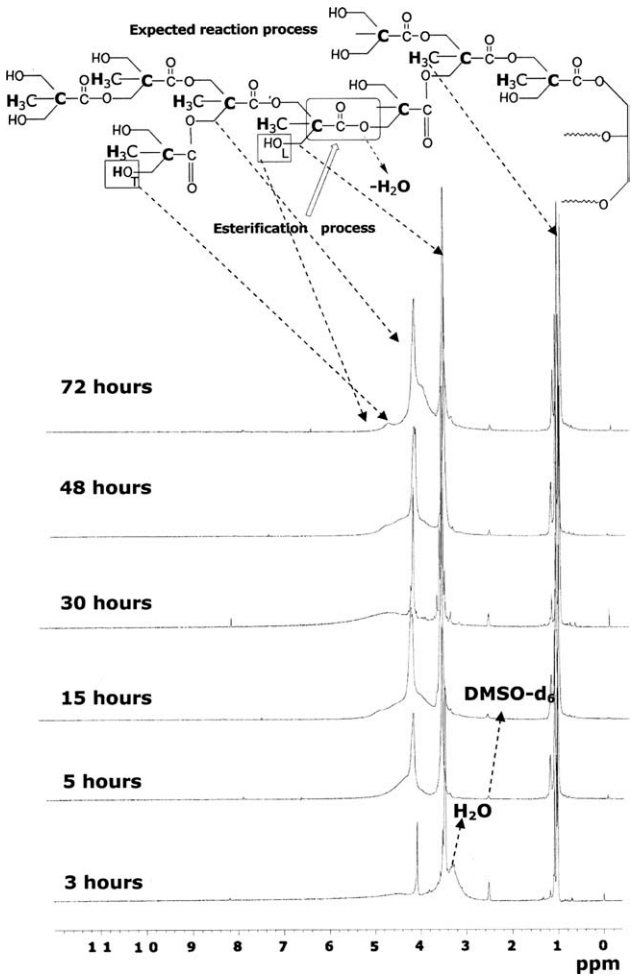

Figure 1 ^{1}H-NMR spectra of the different HBPs (3–72 h).

DB

Molecular weight, PDI, and functionality are three major parameters in HBPs. DB is a special and important parameter, which can be used to analyze differences in the structure and can be calculated from ^{1}H-NMR and ^{13}C-NMR spectra by comparison of the integrals of the different units (D, T, and L) in the HBPs. The DB values of the polyesters were calculated with the Frey and Frechet equations,[28,29] and the data are reported in Table II:

$$DB_{Frey} = (2D/2D + L) \quad (1)$$

$$DB_{Frechet} = (D + T/D + L + T) \quad (2)$$

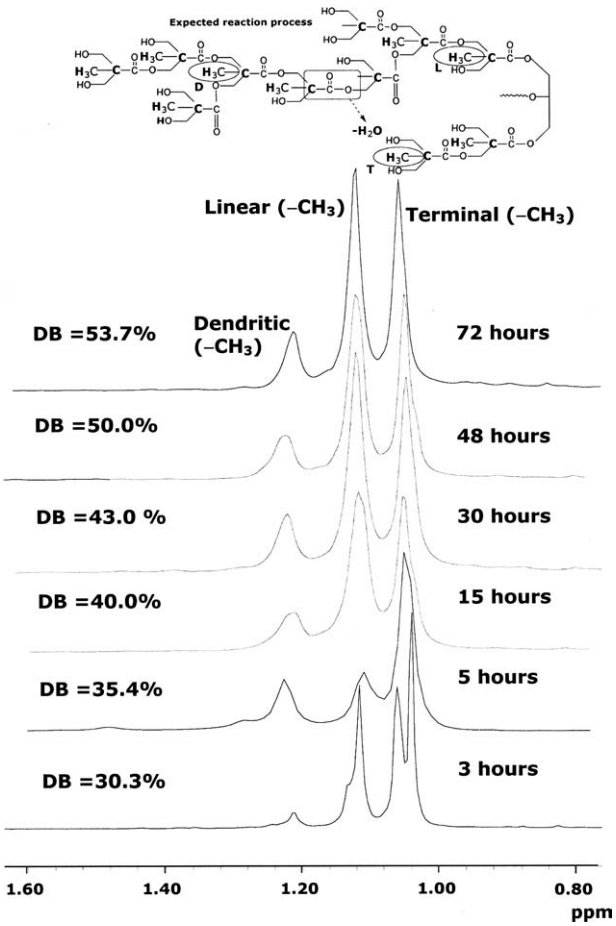

Figure 2 Magnification of the methyl region of the ^{1}H-NMR spectra of HBPs in DMSO-d_6.

NMR analysis

The ^{1}H-NMR spectra of the polyesters together with the chemical shift assignments are shown in Figure 1. As shown, it was possible to distinguish the protons of the —CH_3 groups at 0.99–1.2 ppm from those of the methylene groups attached to reacted hydroxyl groups (—CH_2O—C=O) and unreacted hydroxyl groups (—CH_2OH) resonating at 4.17 and 3.50 ppm, respectively. The signal of CH_2OH was not well separated from that of water, which resonated at 3.32 ppm. The T (—OH) and L (—OH) groups resonated at 4.64 and 4.8 ppm, respectively. Figure 2 shows the magnified methyl region of the ^{1}H-NMR spectra of the HBPs in DMSO-d_6 with DB values. Figure 3 shows the ^{13}C-NMR spectra of HB polyesters. Peaks were observed at 172–175 ppm for carbonyl groups, 63–66 ppm for methylene groups, 46–51 ppm for quaternary carbons, and 15–19 ppm for methyl groups. From the ^{13}C-NMR spectra of the HBPs, the DB was calculated by comparison of the integral values of the different repeating units, that is, the T, L, and D units, to determine their relative amounts. Figure 4 shows the expansion of the quaternary carbon region of the ^{13}C-NMR spectrum of the HBPs. The peaks of the T, D, and L repeat units were

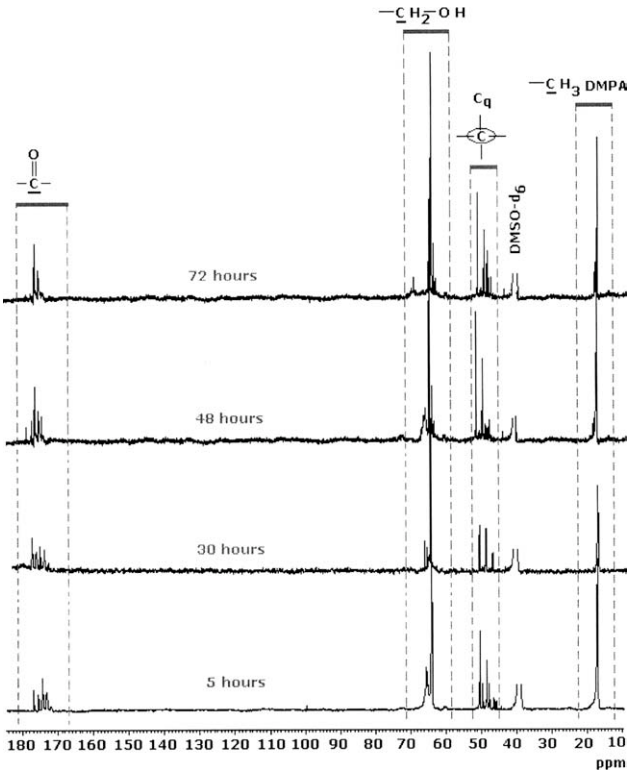

Figure 3 ^{13}C-NMR spectra of the HBPs in DMSO-d_6.

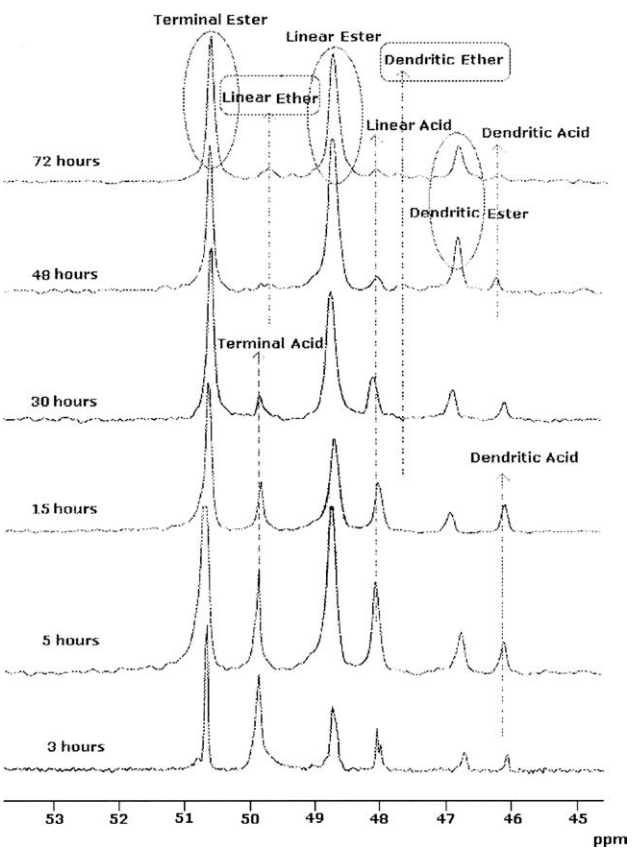

Figure 4 Expansion of the quaternary carbon region of the ^{13}C-NMR spectrum of HBPs (3–72 h). The peaks of the T, D, and L repeat units were all present along with their acid-functional repeat units.

TABLE III
Contents of the D, L, and T Repeat Units of the HBPs Along with Their Focal Point Acid Units as Determined from ^{13}C-NMR

Sample	T_{ester} (%)	T_{acid} (%)	L_{ester} (%)	L_{acid} (%)	D_{acid} (%)	D_{ester} (%)
3 h	33.52	12.61	39.31	7.01	4.04	3.21
5 h	32.73	11.99	39.12	6.81	6.08	3.01
15 h	32.35	11.76	38.23	5.88	8.82	2.94
30 h	33.71	9.66	37.81	4.68	9.72	2.53
48 h	37.61	4.83	37.04	3.02	15.48	1.79
72 h	38.93	0	36.16	1.87	20.89	1.61

present, along with their acid-functional repeat units. The signals of the quaternary carbon belonging to the T, L, and D units resonated at δ's of 50.3, 48.3, and 46.3 ppm, respectively. The corresponding T_{acid}, L_{acid}, and D_{acid} units resonated at δ's of 49.8, 48.0, and 46.1 ppm, respectively.[27,30–33] The integrated intensities of the signals, which correspond to the different repeating units in the quaternary carbons zone, according to Magnusson et al.,[5] are listed in Table III.

^{13}C-NMR spectra of the quaternary carbon of the fifth-generation HBPs at different reaction times from 3 to 72 h are shown in Figure 4. The result suggests that the signal at a δ value of 49.8 ppm belonging to δ_T (acid) disappeared at 72 h of reaction. However, at the same time, new structural units, such as L_{ether} and D_{ether}, were formed along with the T_{ester}, L_{ester}, and D_{ester} units. An interesting observation, shown in Table III, was that the percentage of δ_L (acid) and δ_D (acid) units decreased with increasing reaction time. New signals resonated at 49.3 ppm (L_{ether}) and 47.3 ppm (D_{ether}) because of the formation of ether bonds in the HB structure, and the intensity of the peaks increased with time.[4,33] L_{ether} formed because of the reaction between T —OH groups, and D_{ether} formed because of the reaction between free —OH of L_{ester} with another OH group. Both etherifications could be observed because of intramolecular reaction (cyclic structure inside the HBP) or intermolecular reaction (which increased the molar mass of the polyesters). In fifth-generation polyesters, we observed the increase in ether groups (L_{ether} and D_{ether}) and D unit peak intensity with increasing reaction time. From the NMR analysis, we expected the presence of a cyclic structure in the polyesters because of the formation of L_{ether}.

MALDI-TOF mass spectrometry analysis

MALDI-TOF mass spectrometry is an useful tool for analyzing HB polymers because this can be achieved by a better understanding of the effects of the polymer structure on the physical properties. This can provide information about repeating units, the role of cyclization, and DP. Successive condensation reactions occurred by the loss of a single water molecule in each step. In the mass spectra of the polyesters (shown in Fig. 5), peaks that corresponded to every oligomer were located at equal distances that reflected the mass of the polymer repeating unit. These macromolecules could be formed by intermolecular esterification [Scheme 2 (expected chain growth)] or intermolecular etherification (side product). Intermolecular etherification has a major role in increasing the molar mass of the macromolecule (Scheme 3). In the case of polyesters [with or without a core molecule (Scheme 1)], this method is mostly used as a powerful technique to verify the presence of cyclic structures by comparison of the m/z values with the possible products. The MALDI-TOF mass spectra of the HBPs prepared from GLY and Bis-MPA at different time intervals are shown in Figure 5. The signals of the polyesters were arranged at intervals of $m/z = 116$ Da (the spacing between peaks or mass progression) from each other, which corresponded to $M_{bis\text{-}MPA} - M_{water}$, where M indicates the respective observed series of mass peaks in the MALDI-TOF mass spectra. The mass spectra of the HBPs showed a clear distribution of oligomers with increasing degree of polymerization. The major mass distribution of the HBPs could be written as $m/z = 92 + 23 + 116n$, where n is the number of repeat units, and varied from 2 to 17 for 5 h [Fig. 5(a)], 2–20 for 15 h [Fig. 5(b)], and 7–24 for 30 h [Fig. 5(c)]. The peaks for $[(M_{Bis\text{-}MPA} - M_{H2O})_n + Na]^+$ and $[(M_{Bis\text{-}MPA} - M_{H2O})_n + K]^+$ ions were observed with a separation of 16 amu between them because the ionization of polymers is generally accomplished by the formation of polymer–metal-ion adducts.[34,35] The mass calculation of major series of oligomeric peaks is shown in the following equations:

$$\begin{aligned} M_n &= M_{GLY} + n(M_{bis-MPA} - M_{water}) + M_{Na+} \\ &= 92 + n(134 - 18) + 23 \\ &= 92 + n116 + 23 \end{aligned} \quad (3)$$

$$\begin{aligned} M_n &= M_{GLY} + n(M_{bis-MPA} - M_{water}) + M_{K+} \\ &= 92 + n(134 - 18) + 39 \\ &= 92 + n116 + 39 \end{aligned} \quad (4)$$

where M_n indicates number-average molar mass and n is the DP. M_{GLY}, $M_{bis\text{-}MPA}$, and M_{water} indicate the

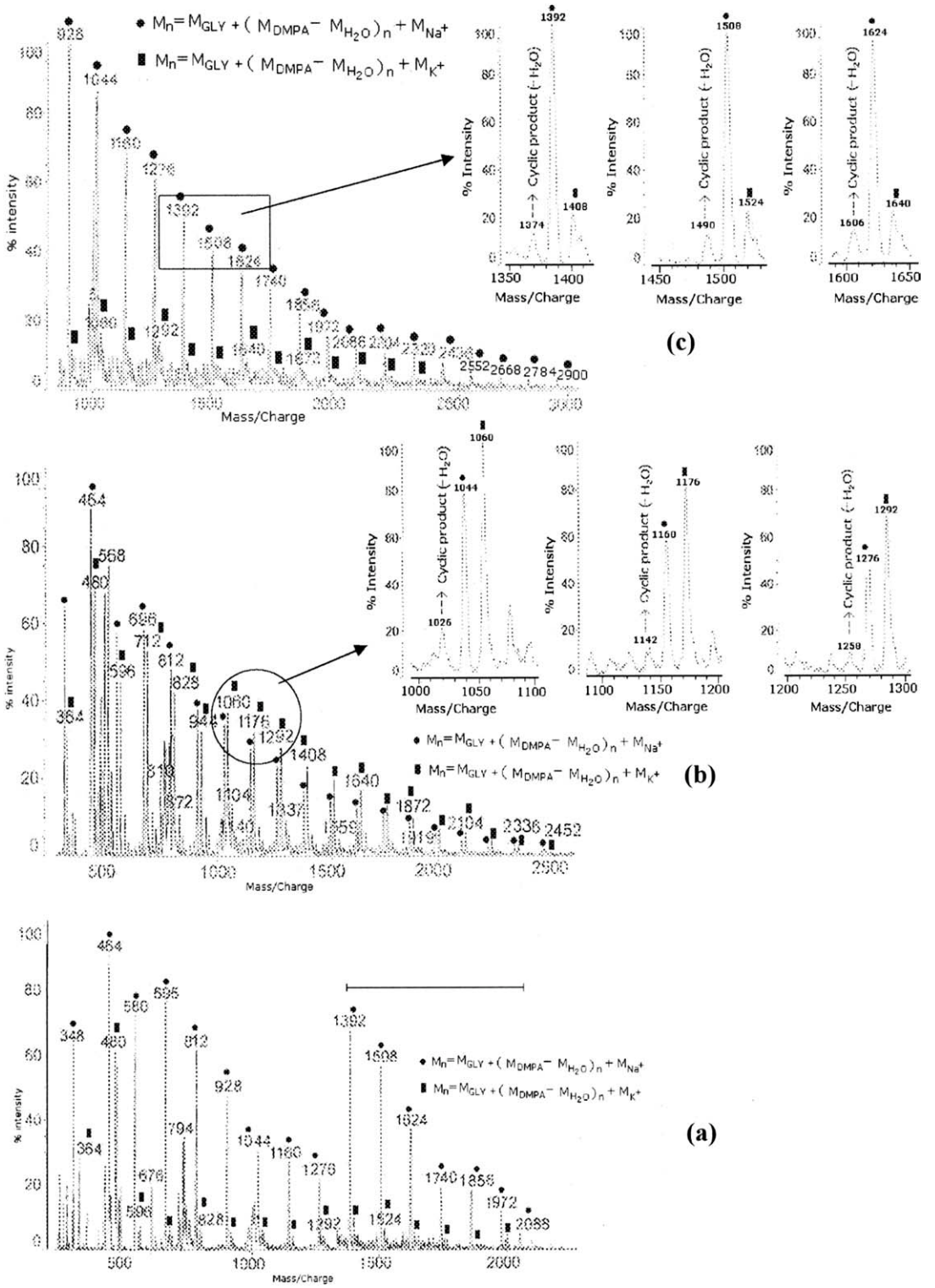

Figure 5 MALDI-TOF MS of HBPs prepared from GLY and bis-MPA (the magnification of the spectra is shown) at (a) 15, (b) 48, and (c) 72 h.

molecular masses of the reactants and water, respectively. The weak peaks located 16 Da above the prominent sodium-cationized ion peaks were due to $[M_{GLY} + n \times (M_{bis\text{-}MPA} - M_{Water}) + K]^+$ ions. Here, no cation salts were added to the HBPs, but the samples were ready to form both sodium and potassium adducts because of the high affinity of HBPs with alkali salt and the traces of sodium and potassium coming from the matrix. In addition to the main peaks, a series of other peaks of lower intensity was also detected, which was ascribed to the cyclized species; these were observed to be more

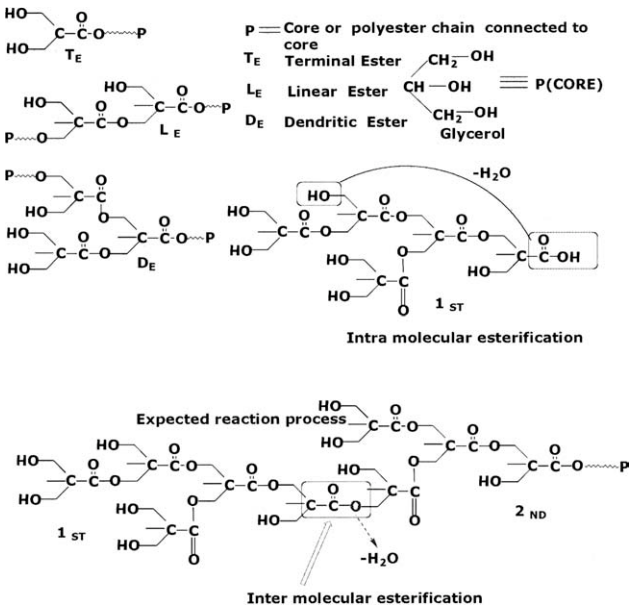

Scheme 2 Different structures generated during the HBP synthesis (intramolecular esterification and intermolecular esterification).

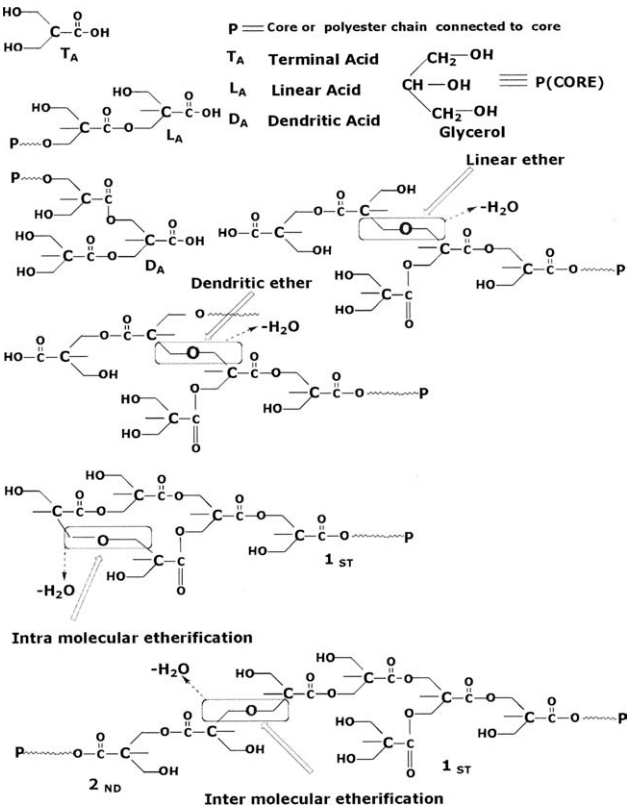

Scheme 3 Different structures including cyclic molecules generated during HBP synthesis (intramolecular etherification and intermolecular etherification).

prominent with increasing reaction time.[27,7,36,37] DP was calculated from the *n* values, and the data of the polyesters are reported in Table IV. A minor series of peaks was observed 18 Da behind the main series, and these are shown in Figure 5(b,c; expanded zone). This was attributed to the loss of a further single water moiety to form a cyclic polymer. A small number of cyclic structures formed in the polyesters could have been due to either intramolecular esterification reactions (Scheme 2) or intramolecular etherification reactions (Scheme 3).[38]

TABLE IV
Molecular Weight Data Obtained for the Sodium- and Potassium-Cationized Oligomers of the HBPs (AB_2 + Core) Fractions from the Respective MALDI Mass Spectra

	After 5 h			After 15 h			After 30 h		
Sample	*n*	Na+	K+	*n*	Na+	K+	*n*	Na+	K+
1	2	348	364	2	348	364	7	928	944
2	3	464	480	3	464	480	8	1044	1060
3	4	580	596	4	580	596	9	1160	1176
4	5	696	712	5	696	712	10	1276	1292
5	6	812	828	6	812	828	11	1392	1408
6	7	928	944	7	928	944	12	1508	1524
7	8	1044	1060	8	1044	1060	13	1624	1640
8	9	1160	1176	9	1160	1176	14	1740	1756
9	10	1276	1292	10	1276	1292	15	1856	1872
10	11	1392	1408	11	1392	1408	16	1972	1988
11	12	1508	1524	12	1508	1524	17	2088	2104
12	13	1624	1640	13	1624	1640	18	2204	2220
13	14	1740	1756	14	1740	1756	19	2320	2336
14	15	1856	1872	15	1856	1872	20	2436	2452
15	16	1972	1988	16	1972	1988	21	2552	2568
16	17	2088	2104	17	2088	2104	22	2668	2684
17				18	2204	2220	23	2784	2800
18				19	2320	2336	24	2900	2916
19				20	2436	2452			

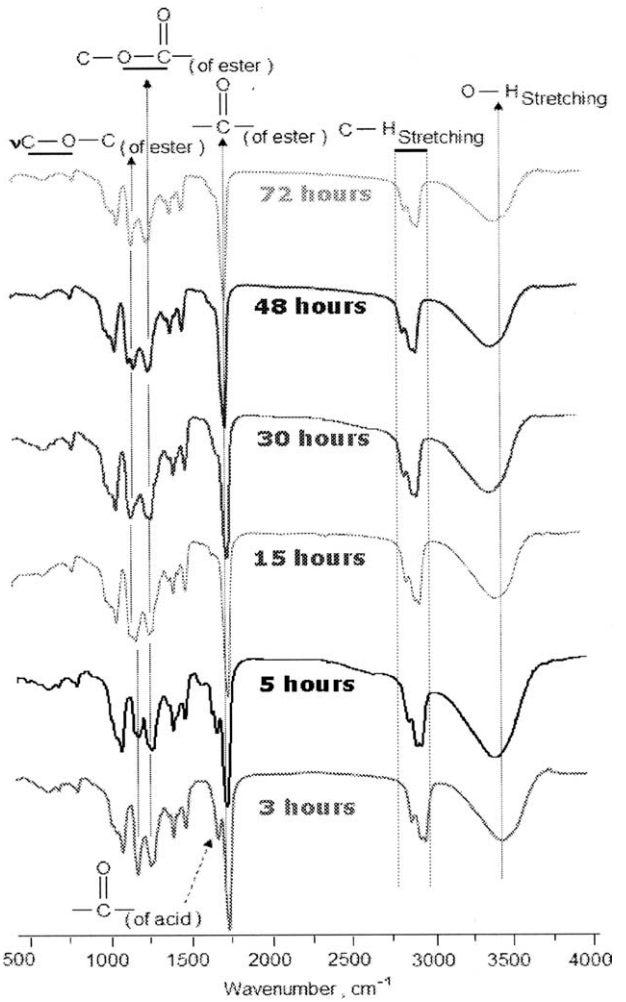

Figure 6 FTIR spectra of the HBPs recorded at room temperature.

IR spectra of the HBPs

FTIR spectroscopy is used extensively to study hydrogen-bonding interactions present in polymer samples and has been demonstrated as a powerful tool in identifying the extent of hydrogen bonding.[39–44] Figure 6 shows the FTIR spectra of the HBPs prepared at different time intervals. In this study, the FTIR experiment was performed to determine the type of hydrogen bonding and the structure–property relationships of the HBPs. The strong absorption band in the range 3250–3500 cm^{-1} for —OH indicated the presence of large numbers of hydroxyl groups on the surface of the HBPs. The carboxyl acid peak of bis-MPA shifted slowly from 1683 to 1721 cm^{-1} with increasing reaction time with the formation of the ester functional. The formation of strong hydrogen-bonding structures and the presence of free —OH groups in these polyesters were the main cause for the broadening of the peaks. This also depended on the distribution of bonded —OH groups; different environments, distances, and geometries would induce a change in the force constant of the —OH groups.[44,45] The spectra of the polyesters were similar, except for the very broad and intense hydroxyl peak. The ester carbonyl stretching vibrations (νC=O) between 1600 and 1800 cm^{-1} were composed of free and hydrogen-bonded carbonyls. The vibration of methyls and methylene groups attached to the quaternary carbon of DMPA in the HBP resulted in antisymmetric ($\nu_{as}CH_3$) and symmetric (ν_sCH_3) stretching of the methyl groups at 2948 and 2868 cm^{-1}, respectively. The other bands at 2906 and 2835 cm^{-1} belonged to the antisymmetric ($\nu_{as}CH_2$) and symmetric (ν_sCH_2) stretching of methylene groups, respectively. The peak at 1465 cm^{-1} was due to a CH_3 asymmetric deformation vibration. The C—O stretching and O—H deformation of bis-MPA (COOH groups) appeared at 1226–1250 cm^{-1}, but these peaks were not observed clearly because of the overlap with ester peaks.[27,46]

HB polymers show intermolecular and intramolecular hydrogen-bonding interactions. This hydrogen bonding can affect the chain length, chain packing, rigidity, and molecular order.[41–43] The formation of hydrogen bonding in macromolecules decreases the distance among hydroxyl to ester and hydroxyl groups, which also affects the properties. Hydrogen bonding is characterized by a shift of frequency to lower wave numbers than those corresponding to free groups (i.e., no hydrogen bonding). The H-bonding strength estimates the extent of the frequency shift. To obtain information about the nature of hydrogen bonding in the polyesters at room temperature, we deconvoluted the —OH region. Figure 7(a–c) shows the hydrogen bonding between molecular segments of the same HBP molecule (intramolecular) or between neighboring HBP molecules (intermolecular). Hydrogen bonding can be expected as a result of the interaction between hydroxyl groups or carbonyl groups having a proton acceptor characteristic and the hydroxyl end groups. The observed bands at 3271, 3330, 3405, and 3512 cm^{-1} of the sample after 72 h were due to hydrogen bonding with the esteric C=O—H—O, esteric O=C—O—H—O, intermolecular and intramolecular O—H—O—H, and free O—H, respectively.[27,47] More OH groups were bonded than free OH groups. Figure 7(d–f) shows two bands in the 1600–1800 cm^{-1} zone, which belonged to free and bonded carbonyl groups. The significant changes of the polyester free and bonded bands were attributed mainly to the structural rearrangement of HBP molecules with the existing network of hydrogen bonds between the more electronegative ester groups and O—H groups. Indeed, the hydrogen bonding was formed because of the large number of polar OH groups, which implied a greater possibility of molecular interaction.

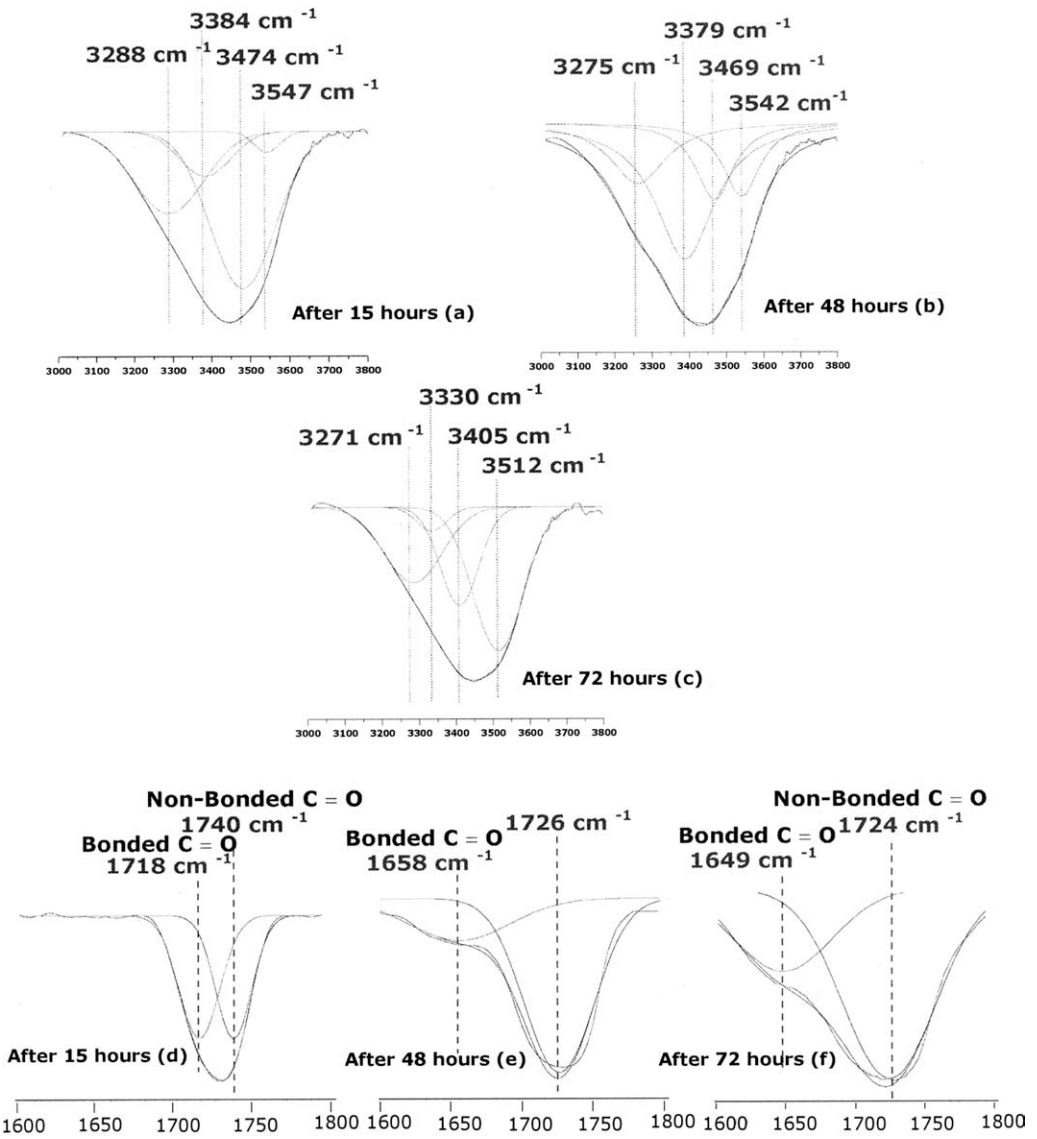

Figure 7 O—H and C=O peak deconvulation of the HBPs.

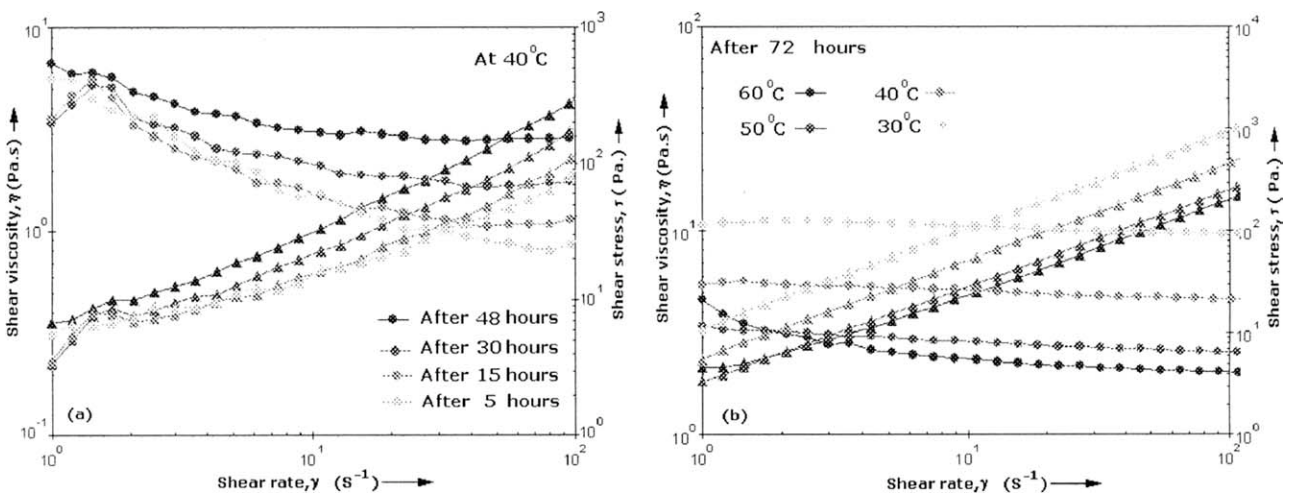

Figure 8 Shear viscosity (η) and shear stress (ι) of HBPs as a function of shear rate at different (a) reaction times and (b) temperatures.

Melt viscosity

In general, factors such as molecular architecture and composition, molecular weight, temperature, and shear rate affect the viscosity of a polymer because the viscosity originates from interactions between the polymer molecules. Moreover, the melt viscosity of a polymer/oligomer is dependent on the segment density within the volume of a molecule and intermolecular chain entanglement. Because of the spherelike structures of the HBPs, there were few entanglements among molecular chains; this resulted in a rather lower viscosity,[48,49] and this is one of the important reasons for the development of these polymers for ecofriendly formulations. Figure 8(a) shows the rheological behavior of the samples after 5, 15, 30, and 48 h. The viscosity for all samples decreased drastically when the shear rate increased from 10 to 10^2. This implied that all of the samples exhibited shear thinning and non-Newtonian flow behavior.[50] The effect of the reaction time of the HBPs on the melt viscosity is also illustrated in Figure 8(a). The melt viscosity of these HBPs followed the following order according to time: 5 h $<$ 15 h $<$ 30 h $<$ 48 h. The increase in the viscosity might have been observed because of the increased molecular weight. Figure 8(b) shows the melt viscosity profiles of HBPs synthesized after 72 h as a function of temperature. This HBP showed Newtonian characteristics at different temperatures; that is, the viscosities were independent of shear rate, which could have been to the lack of entanglement of the HBPs.[51] It is evident from Figure 8(b) that, for all of the samples, the increase in the temperature caused a decrease in their viscosity. The increased temperature led to the orientation of macromolecular chains and destroyed the associated structures, such as hydrogen bonding and chain entanglements; hence, the viscosity decreased.

CONCLUSIONS

A novel synthetic strategy toward the synthesis of fifth-generation HBPs with GLY as a core was adopted. A structural buildup investigation of the HBPs synthesized at different reaction time intervals was carried out by various instrumental techniques. ^{1}H-NMR and ^{13}C-NMR spectroscopy analysis indicated a DB greater than 50%. The intermolecular and intramolecular interaction study with FTIR spectroscopy indicated the pronounced hydrogen bonding in HBPs, which was favored by the presence of OH end groups. The viscosity measurement showed the Newtonian behavior of HBPs with shear rate. From this structural investigation of HBPs, we concluded that, as the reaction time increased for the preparation of HBPs, the three-dimensional spherical shape enlarged in size, and also, more hydroxyl groups attached to its periphery. Because the core molecule used in this study is commercially available in abundance, this signifies wide commercial implications for these HBPs.

References

1. Nasar, A. S.; Jikei, M.; Kakimoto, M. Eur Polym J 2003, 39, 1201.
2. Núñez, E.; Ferrando, C.; Malmström, E.; Claesson, H.; Werner, P. E.; Gedde, U. W. Polymer 2004, 45, 5251.
3. Malmström, E.; Hult, A. Macromolecules 1996, 29, 1222.
4. Malmström, E.; Johansson, M.; Hult, A. Macromolecules 1995, 28, 1698.
5. Magnusson, H.; Malmström, E.; Hult, A. Macromolecules 2000, 33, 3099.
6. Žagar, E.; Žigon, M. Macromolecules 2002, 35, 9913.
7. Burgath, A.; Sunder, A.; Frey, A. Macromol Chem Phys 2000, 201, 782.
8. Linda, C.; Xavier, A.; Celine, G.; Martine, T.; Alain, F. Macromol Symp 2003, 199, 209.
9. Nunez, C. M.; Chiou, B. S.; Andrady, A. L.; Khan, S. A. Macromolecules 2000, 33, 1720.
10. Kim, Y. H.; Webster, O. W. J Am Chem Soc 1990, 112, 4592.
11. Asif, A.; Shi, W.; Shen, X.; Nie, K. Polymer 2005, 46, 11066.
12. Antonitti, A.; Rosenauer, C. Macromolecules 1991, 24, 3434.
13. Mishra, A. K.; Jena, K. K.; Raju, K. V. S. N. Prog Org Coat 2009, 64, 47.
14. de Brabander-van den berg, E. M. M.; Nijenhuis, A.; Mure, M.; Keulen, J.; Reintjens, R.; Vandenbooren, F.; Bosman, B.; Denaat, R.; Frijins, T.; Wal, S. V. D. M.; Castelijns, J. P.; Meijer, E. W. Macromol Symp 1994, 77, 51.
15. Yates, C. R.; Hayes, W. Eur Polym J 2004, 40, 1257.
16. Chattopadhyay, D. K.; Raju, K. V. S. N. Prog Polym Sci 2007, 32, 352.
17. Stumbe, J. F.; Bruchmann, B. Macromol Rapid Commun 2004, 25, 921.
18. Malmstroem, E.; Hult, A. Macromol Chem Phys 1997, 37, 555.
19. Malmstrom, A.; Hult, A.; Gedde, U. W.; Liu, F.; Boyd, R. H. Polymer 1997, 38, 4873.
20. Dušek, K.; Šomvársky, J.; Smrčková, M.; Simonsick, W. J.; Wilczek, L. Polym Bull 1999, 42, 489.
21. Hsieh, T. T.; Tiu, C.; Simon, G. P. Polymer 2001, 42, 1931.
22. Malmström, E.; Liu, F.; Boyd, R. H.; Hult, A.; Gedde, U. W. Polym Bull 1994, 32, 679.
23. Zhu, P. W.; Zheng, S.; Simon, G. Macromol Chem Phys 2001, 202, 3008.
24. Murillo, E. A.; Vallejo, P. P.; Sierra, L.; Lopex, B. L. J Appl Polym Sci 2009, 112, 200.
25. Parker, D.; Feast, W. J. Macromolecules 2001, 34, 2048.
26. Savita, K.; Mishra, A. K.; Chattopadhyay, D. K.; Raju, K. V. S. N. J Polym Sci Part A: Polym Chem 2007, 45, 2673.
27. Jena, K. K.; Raju, K. V. S. N.; Prathab, B.; Aminabhavi, T. M. J Phys Chem B 2007, 111, 8801.
28. Hawker, C. J.; Lee, R.; Frechet, J. M. C. J Am Chem Soc 1991, 113, 4583.
29. Thomasson, D.; Boisson, F.; Girard-Reydet, E.; Mechin, F. React Funct Polym 2006, 66, 1462.
30. Jiang, G.; Wang, L.; Chen, T.; Dong, X.; Yu, H.; Wang, J.; Chen, C. J Polym Sci Part A: Polym Chem 2005, 43, 5554.
31. Komber, H.; Ziemer, A.; Voit, B. Macromolecules 2002, 35, 3514.
32. Jiang, G.; Wang, L.; Yu, H.; Chen, C.; Dong, X.; Chen, T.; Yang, Q. Polymer 2006, 47, 12.

33. Jena, K. K.; Mishra, A. K.; Raju, K. V. S. N. J App Polym Sci 2008, 110, 4022.
34. Mehl, J. T.; Murgasova, R.; Dong, X.; Hercules, D. M.; Nefzger, H. Anal Chem 2000, 72, 2490.
35. Raju, N. P.; Mirza, S. P.; Vairamani, M.; Ramulu, A. R.; Pardhasaradhi, M. Rapid Commun Mass Spectrom 2001, 15, 1879.
36. Feast, W. J.; Keeney, A. J.; Kenwright, A. M.; Parker, D. Chem Commun 1997, 1749.
37. Parker, D.; Feast, W. J. Macromolecules 2001, 34, 5792.
38. Chikh, L.; Tessier, M.; Fradet, A. Polymer 2007, 48, 1884.
39. Wang, C. B.; Coopers, S. L. Macromolecules 1983, 16, 775.
40. Yen, M. S.; Kuo, S. C. J. J App Polym Sci 1996, 61, 1639.
41. Van Heumen, J. D.; Stevens, J. R. Macromolecules 1995, 28, 4268.
42. Wen, T. C.; Wang, Y. J.; Cheng, T. T.; Yang, C. H. Polymer 1999, 40, 3979.
43. Shengquing, X.; Bin, C.; Tao, T.; Baotang, H. Polymer 1999, 40, 3399.
44. Win, T. C.; Fang, J. C.; Yang, C. H. J App Polym Sci 2001, 82, 389.
45. Mikhaylova, Y.; Adam, G.; Haussler, L.; Eichhorn, K. J.; Voit, B. J Mol Struct 2006, 788, 80.
46. Zagar, E.; Grdadolnik, J. J Mol Struct 2003, 658, 143.
47. Jena, K. K.; Raju, K. V. S. N. Ind Eng Chem Res 2008, 47, 9214.
48. Sendijarevic, I.; McHugh, A. J. Macromolecules 2000, 33, 590.
49. Jena, K. K.; Raju, K. V. S. N. Ind Eng Chem Res 2007, 46, 6408.
50. Savita, K.; Mishra, A. K.; Krishna, A. V. R.; Raju, K. V. S. N. Prog Org Coat 2007, 60, 52.
51. Vukovic, J.; Lechner, M. D.; Jovanovic, S. Macromol Chem Phys 2007, 208, 2321.